RSC Advances

PAPER

View Article Online
View Journal | View Issue

Cite this: *RSC Adv.*, 2025, **15**, 8315

Selective oxidation of benzyl ethers to esters catalyzed by Cu_2O/C_3N_4 with TBHP & oxygen as co-oxidants†

Li Zhu,*[a] Xiyu Niu[b] and Xiaoquan Yao *[b]

A novel cuprous oxide carbon nitrogen composite material, Cu_2O/C_3N_4, was designed and successfully synthesized. This nanocomposite exhibited superior catalytic performance in the selective oxidation of benzyl ethers to benzoates. Remarkably, the catalytic reaction proceeded efficiently at room temperature in an acetone solution, achieving good to excellent yields for various substrates. Notably, only 1.5 equivalents of TBHP were necessary for this reaction, which is below the stoichiometric requirement. Mechanistic studies revealed that oxygen in air collaborates with TBHP as a co-oxidant. Compared to prior research, the oxidation of benzyl ethers catalyzed by Cu_2O/C_3N_4 offers not only a lower reaction temperature and simpler procedure but also a significant reduction in the required amount of TBHP.

Received 29th October 2024
Accepted 6th March 2025

DOI: 10.1039/d4ra07724e

rsc.li/rsc-advances

Introduction

Aromatic esters are crucial structural units in many chemical products, including medicines, spices, and preservatives. They also serve as important intermediates and solvents in many organic synthesis processes.[1] Traditionally, aromatic esters can be synthesized through esterification and transesterification. They can also be obtained through the synthesis of acid chloride and acid anhydride.[2–4] Despite the simple and easy availability of raw materials, the above reactions usually suffer from some unavoidable problems, such as prolonged heating reflux or the use of highly hygroscopic substrates. Therefore, efforts have been made to develop new synthetic methods for the preparation of esters, among which the direct oxidation of benzyl ethers may provide a new low-cost and environmentally friendly alternative for the synthesis of aromatic esters.[5]

In recent years, many efficient catalysts as well as many oxidants,[5] have been reported for the direct oxidation of benzyl ethers to esters. Among the reported examples, undoubtedly, heterogeneous catalytic systems provide higher efficiency and sustainability compared to the homogeneous catalytic reactions.[6] In 2016, Ahmad Shaabani[6a] and his coworkers developed a hydroxyapatite-supported cobalt catalyst, Co-NHAp, and successfully utilized as an efficent catalyst for the oxidation of benzocyclic ether to lactone at 100 °C (Scheme 1a). In 2017, with the Eosin Y-sensitized titanium dioxide as photocatalyst, Cong's group developed an efficient aerobic photooxidation of benzyl ethers to benzoates (Scheme 1b).[6b] Subsequently, in 2019, a catalytic oxidation of benzylic ethers to esters was developed by Gao's group utilizing reusable MnO*x*-N@C as catalyst and *tert*-butyl hydroperoxide (TBHP) as benign oxidant under neat condition at 60 °C for 24 h (Scheme 1c).[6c]

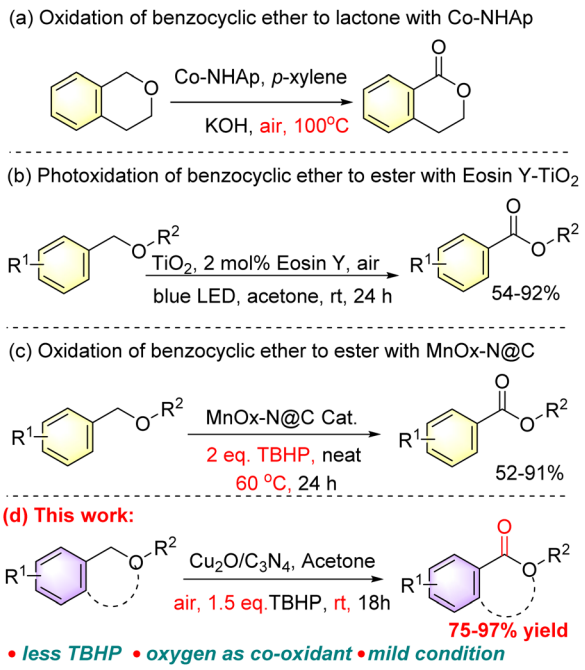

Scheme 1 Selective oxidation of benzyl ethers to benzoates.

[a]Department of Chemistry, School of Pharmacy, Nanjing Medical University, Nanjing 211166, P. R. China. E-mail: zl9422@njmu.edu.cn
[b]Department of Applied Chemistry, School of Material Science and Technology, Nanjing University of Aeronautics and Astronautics, Nanjing 210016, P. R. China. E-mail: yaoxq@nuaa.edu.cn

† Electronic supplementary information (ESI) available. See DOI: https://doi.org/10.1039/d4ra07724e

As a kind of novel superior materials, N-doped carbon materials (N–C material) have been wildly used in many fields such as electrode materials and photocatalysts *etc.*,[7] and there are also many reports in organic synthesis.[8] Based on our group's continuous efforts in the field of Cu–N–C material catalysed oxidation,[9] oxidative coupling[10] and photocatalytic reactions,[11] we hope to report here a new cuprous oxide–carbon nitride composite, Cu_2O/C_3N_4, which has been successfully utilized as a highly efficient catalyst for the selective oxidation of benzyl ethers to benzoates (Scheme 1d). The oxidation of benzyl ether worked smoothly at room temperature and gave 75–97% yield for various substrates in acetone solution. It is worth mentioning that only 1.5 equiv. of TBHP, which is less than the stoichiometric amount, was required. The mechanism investigation showed that the oxygen in air works as co-oxidant with TBHP. Compared with previous work, the present Cu_2O/C_3N_4-catalyzed oxidation of benzyl ethers not only has the advantages of lower reaction temperature and easier operational procedures, but also substantially decreases the required amount of TBHP.

Experimental

The synthesis of $Cu_2O/g\text{-}C_3N_4$

Under a nitrogen atmosphere, 100 mL of distilled water and 26.3 mg of polyethylene glycol 400 (approximately 22 μL) were introduced into a 500 mL three-necked flask. The mixture was stirred until the polyethylene glycol fully dissolved. Subsequently, 500.0 mg of hydrated copper acetate (2.5 mmol) and 1.4400 g of $g\text{-}C_3N_4$ material were added to the flask. The resultant mixture was then stirred at 30 °C for 10 minutes. While stirring vigorously, 8.5 mL of 0.6 M sodium hydroxide aqueous solution was incorporated and allowed to react for an additional 20 minutes. Following this, 0.75 mL of 2 M hydrazine hydrate aqueous solution was gradually introduced. As the hydrazine hydrate was added, the blue-green reaction solution transitioned to a red-brown hue. After a continuous stirring period of 5 hours, the mixture was left to settle for 10 minutes, during which time reddish-brown solid precipitates formed at the flask's bottom. The Cu_2O/C_3N_4 (20 wt%) catalyst, appearing as a reddish-brown powder, was subsequently harvested *via* centrifugation. The powder was then washed in succession with distilled water, anhydrous ethanol, and anhydrous diethyl ether (each wash involved 5 mL × 3). Finally, the powder was dried in a vacuum oven at 50 °C for a duration of 6 hours.

General procedure for the synthesis of 2

In a Schlenk tube connected to an air balloon, add 10 mol% (13.40 mg) of Cu_2O/C_3N_4 catalyst, 0.2 mmol of benzyl methyl ether (**1a**), 0.3 mmol of TBHP (70 wt% in H_2O), and 1 mL of acetone. Allow the mixture to react at room temperature for 18 hours. After completion, filter off the catalyst and analyze the conversion rate and selectivity using gas chromatography. Purify the reaction mixture by flash column chromatography on silica gel using a petroleum ether : ethyl acetate ratio of 20 : 1. The desired product, compound **2a**, is obtained in an 88% yield.

Results and discussion

The Cu_2O/C_3N_4 composite material was prepared by liquid phase reduction of $Cu(OAc)_2$ with $N_2H_4 \cdot H_2O$ as the reducing agent in an aqueous suspension of $g\text{-}C_3N_4$ obtained by calcination method using melamine as the raw material (for the image of $g\text{-}C_3N_4$, please see Fig. S1 in ESI†).

Firstly, the morphology of the nanocomposite was characterized by TEM (Fig. 1). As can be seen in Fig. 1, C_3N_4 has a lamellar structure, and Cu_2O with a particle size of 200–400 nm and a cubic structure is uniformly distributed in it.[12]

An XRD analysis test on Cu_2O/C_3N_4 was then conducted and compared with $g\text{-}C_3N_4$. As shown in Fig. 2, the $g\text{-}C_3N_4$ calcined from melamine at high temperature has diffraction peaks at 27.3° and 12.8°, which are the diffraction peaks of (002) and (100) crystal planes, indicating that there are triazine units in our synthesized samples. In the XRD diffraction pattern of Cu_2O/C_3N_4, in addition to the two diffraction peaks of $g\text{-}C_3N_4$, the diffraction peaks of Cu_2O nanoparticles at 29.6°, 36.5°, 42.3°, 61.4°, 73.6° and 77.4° can also be observed. These peaks belong to the diffraction peaks of cubic Cu_2O crystals on (110), (111), (200), (220), (311), (222) crystal planes, respectively.[12–14]

Fig. 3 shows the XPS analysis of the Cu_2O/C_3N_4 nanocomposite. The full spectrum a shows that Cu_2O/C_3N_4 is composed of four elements: C, N, O, and Cu (Fig. 3a). Fig. 3b shows the XPS spectrum of C 1s and there are three signal peaks at 288 eV, 286.7 eV and 284.5 eV. The characteristic peak at 288 eV is the carbon on the aromatic ring of the C_3N_4 triazine ring, which is bonded to the amino group outside the aromatic ring. The peak at 286.7 eV indicates the C=N bond on the structure of the C_3N_4 triazine ring. The signal peak at 284.5 eV

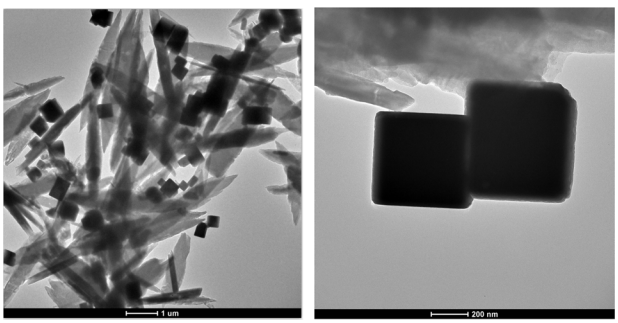

Fig. 1 TEM images of Cu_2O/C_3N_4.

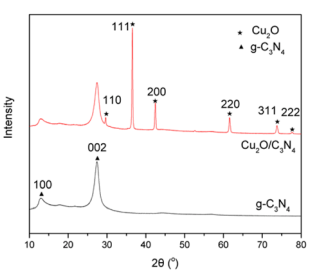

Fig. 2 XRD of $g\text{-}C_3N_4$ and Cu_2O/C_3N_4.

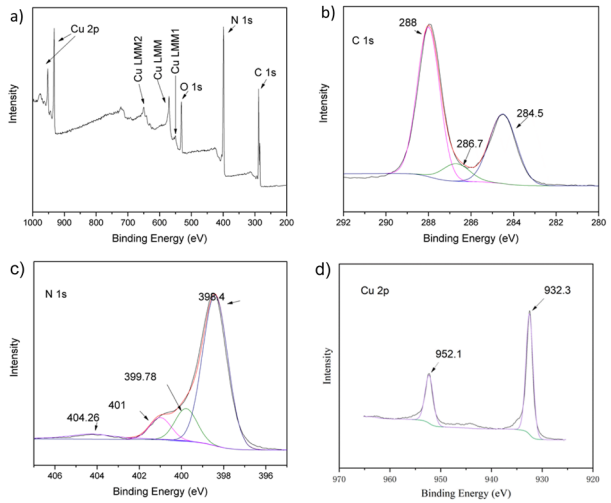

Fig. 3 The XPS spectrum of Cu_2O/C_3N_4: (a) survey, (b) N 1s, (c) C 1s, (d) Cu 2p.

indicates that the material has a C=C double bond.[13] Fig. 3c is the high resolution spectrum of N 1s, which is mainly divided into four peaks. The peaks at 398.4 and 399.78 eV are attributed to pyridine and graphitic nitrogen. The weak peak at 401 eV indicates the presence of amino groups (C–N–H), and the signal peak at 404.26 eV belongs to N–O on carbon–nitrogen materials.[13–15] Fig. 3d is the high resolution spectrum of Cu 2p orbital. There are two characteristic peaks at 952.1 eV and 932.2 eV. According to literature reports, the two bond energy peaks represent the orbital peaks of Cu $2p_{1/2}$ and Cu $2p_{3/2}$ respectively. The two peaks are characteristic of Cu^+ in Cu_2O, in line with the literature reports.[14]

With the Cu_2O/C_3N_4 composite in hand, the selective oxidation of benzyl methyl ether (**1a**) to methyl benzoate (**2a**) was selected as prototype to start our investigation for the optimized reaction conditions, and the data were summarized in Table 1.

Initially, using 10 mol% of Cu_2O/C_3N_4 as the catalyst, benzyl methyl ether (**1**) was smoothly transformed into methyl benzoate (**2**) with a 93% conversion and a >99% selectivity in air, employed 1.5 equiv. of TBHP (70% wt% in H_2O) as an oxidant (entry 1, Table 1). As a control experiment, almost no reaction occurred in the absence of catalyst (entry 2). g-C_3N_4 showed limited catalytic activity with a 17% conversion (entry 3). When Cu_2O, Cu or CuO NPs were used as catalysts respectively, only moderate conversions but excellent selectivities were obtained, in which Cu_2O gave the best result (entries 4–6). Obviously, the combination of Cu_2O and g-C_3N_4 improve significantly the catalytic efficiency of the reaction (entry 1 *vs.* entry 4).

In theory, since alkylhydroperoxides function as mono-oxygen donors, two equivalents of TBHP should be necessary for the stoichiometric reaction.[5e] The current result substantially

Table 1 Optimization of reaction conditions[a]

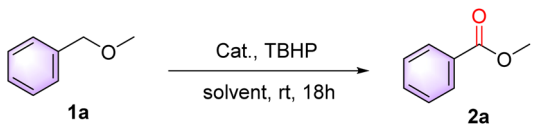

1a 2a

Entry	Catalyst	Solvent	TBHP (equiv.)	Conv.[b] (%)	Sel.[b] (%)	Yield[b] (%)
1	Cu_2O/C_3N_4	Acetone	1.5	93	99	93
2	—	Acetone	1.5	Trace	—	Trace
3	g-C_3N_4	Acetone	1.5	17	99	17
4	Cu_2O	Acetone	1.5	63	96	60
5	CuO	Acetone	1.5	35	98	34
6	Cu	Acetone	1.5	53	98	52
7[c]	Cu_2O/C_3N_4	Acetone	1.5	56	99	56
8[d]	Cu_2O/C_3N_4	Acetone	0	Trace	—	Trace
9	Cu_2O/C_3N_4	Acetone	0.1	17	94	16
10	Cu_2O/C_3N_4	Acetone	0.2	47	87	41
11	Cu_2O/C_3N_4	Acetone	1	67	94	63
12	Cu_2O/C_3N_4	Acetone	2	90	95	85
13[d]	Cu_2O/C_3N_4	Acetone	1.5	88	99	88
14[e]	Cu_2O/C_3N_4	Acetone	1.5	90	91	81
15	Cu_2O/C_3N_4	CH_2Cl_2	1.5	95	45	42
16	Cu_2O/C_3N_4	THF	1.5	30	53	16
17	Cu_2O/C_3N_4	EtOH	1.5	100	9	9
18	Cu_2O/C_3N_4	CH_3CN	1.5	91	85	77
19	Cu_2O/C_3N_4	Dioxane	1.5	53	99	53
20	Cu_2O/C_3N_4	H_2O	1.5	Trace	—	Trace
21	Cu_2O/C_3N_4	DMF	1.5	Trace	—	Trace

[a] Reaction conditions: **1a** (0.20 mmol), solvent (1.0 mL), catalyst 10 mol%, TBHP (70% wt% in H_2O), at room temperature in air for 18 h. [b] Analysed by GC. [c] Under N_2 atmosphere. [d] In 1 atm. of O_2. [e] At 60 °C.

decreases the required amount of TBHP and suggests that atmospheric oxygen might play a role in the reaction (comparison with previous reports, see Table S2 in ESI†). To further investigate the actual source of oxidant in the reaction, several controlled experiments were conducted (entries 7–13). First, we performed the reaction under a nitrogen atmosphere (entry 7). Notably, the conversion dropped significantly to 56%, yet the selectivity remained high at 99%. However, without TBHP, only a trace amount of conversion was detected under 1 atm of oxygen (entry 8). These results suggest that oxygen works in synergy with TBHP, both contributing to the oxidation process. Based on this hypothesis, we tested loadings of 0.1, 0.2, and 1 equivalent of TBHP (entries 9, 10 and 11, respectively). Although the conversions were only 17%, 47%, and 67% respectively, these experiments further validated the cooperative role of oxygen as a co-oxidant. When 2 equivalents of TBHP were employed, there was a slight decrease in both conversion and selectivity (entry 1 *vs.* entry 12). Additionally, we attempted the reaction in an oxygen-rich environment with 1.5 equivalents of TBHP, but this resulted in a slightly reduced conversion (entry 13).

Furthermore, the reaction was conducted at 60 °C, which notably decreased the selectivity towards methyl benzoate (entry 14). Additionally, a range of alternative solvents were evaluated. Acetone clearly emerged as the optimal solvent choice among those tested (entry 1 *vs.* entries 15–21).

Following the optimized conditions (entry 1, Table 1), we proceeded to investigate the substrate scope as presented in Scheme 2. We were pleased to discover that various benzyl ethers underwent smooth reactions under the standardized conditions, yielding the corresponding benzyl esters in good to excellent yields.

Firstly, the influence of substitutions on the aromatic ring of benzyl methyl ether was investigated. When various substituents were introduced at the *para*-position relative to the ether bond, it was observed that both electron-donating and electron-withdrawing groups resulted in similar isolated yields (80–82%), albeit these yields were lower than that of the non-substituted compound **1a** (**2a** *vs.* **2b–2f**, Scheme 2).

Interestingly, substitutions at the *meta*-position appear to influence the reaction differently. When substituents like Me-, MeO-, and Cl- were present at the *meta*-position, yields ranging from 86–88% were achieved for compounds **2g–2i**. However, the introduction of strong electron-withdrawing groups, such as F- and NO_2-, led to a significant decrease in yield, with 75% of compound **2j** and 80% of **2k** being isolated, respectively. Furthermore, *ortho*-subsitituted substrates also gave the corresponding product **2l–2n** with good yields around 80%. It is noteworthy that the selectivity for products **2a–2j** is consistently above 98% (please see Table S1, ESI† for more details).

Utilizing the current procedure, several disubstituted benzoates were synthesized from the corresponding benzyl ethers, resulting in products **2o–2s** with yields ranging from 78–87%. Notably, the best result was obtained with the dimethoxyl-substituted substrate **1q**.

In addition to benzyl methyl ether, we extended our studies to other benzyl ethers. Isochroman, a cyclic benzyl ether,

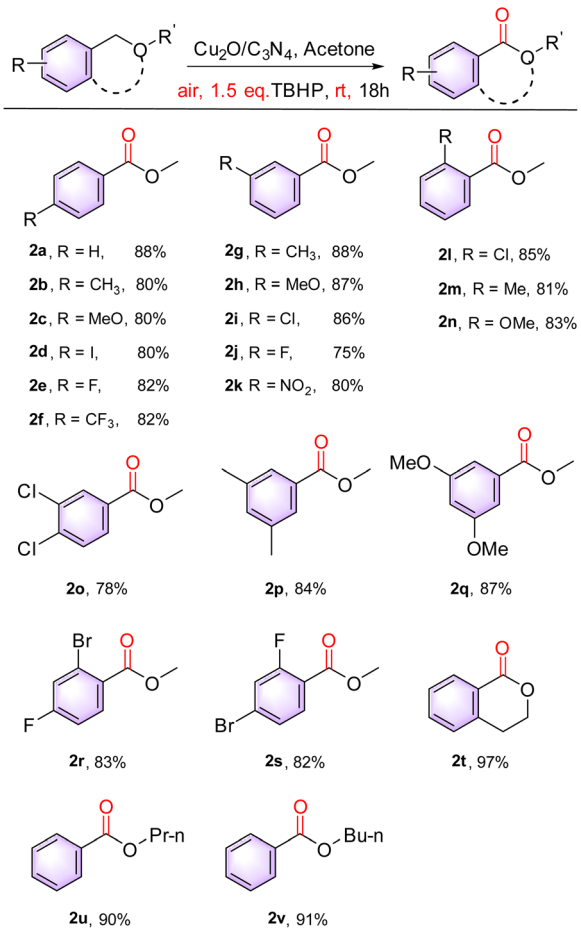

Scheme 2 Scope exploration of the substrates: substrate **1** (0.20 mmol), solvent (1.0 mL), catalyst 10% mol, TBHP (70 wt% in H_2O) 0.3 mmol, at room temperature in air for 18 h; isolated yield.

exhibited exceptional reactivity, achieving an excellent yield of up to 97% in its oxidation product **2t.** Furthermore, our investigation into benzyl fatty ethers included benzyl propyl ether and benzyl butyl ether, both of which underwent oxidation with high efficiency, producing compounds **2u** and **2v** in yields of 90% and 91%, respectively.

Furthermore, to investigate the practical applicability of this protocol was performed using the reaction of **1a** (10 mmol), resulting in the desired product **2a** with a 76% yield (Scheme 3).

As a heterogeneous catalyst, the Cu_2O/C_3N_4 nanocomposite can be conveniently separated and recovered from the reaction mixture *via* centrifugation. After sequential washing with ethanol and ether, fresh substrates and solvent are added to initiate a new reaction cycle. By following this procedure, the

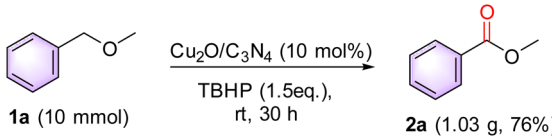

Scheme 3 A gram scale of the reaction of **1a** to **2a**.

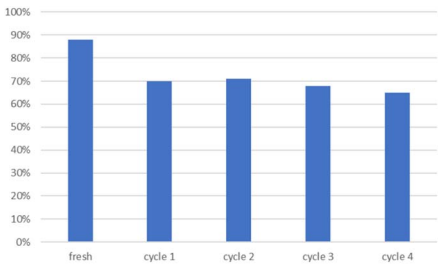

Scheme 4 The recyclability of Cu_2O/C_3N_4 with the reaction of **1a** to **2a**.

catalyst was effectively recycled, and the results are summarized in Scheme 4. It was observed that the yields from cycles 1 to 4 were similar but significantly lower than that obtained with the fresh catalyst. This reduction in activity may be attributed to the partial detachment of Cu_2O nanoparticles from the Cu_2O/C_3N_4 composite during the initial washing process.

In prior optimization studies (entries 7–13, Table 1), we confirmed that oxygen in air functions as an aiding oxidant alongside TBHP in the catalytic oxidation process, while TBHP also triggers the oxidation process. In 2018, our group reported on a ball-milled Co–N–C nanocomposite that catalyzes the oxidation of benzylic C–H bonds to ketones.[16] Notably, the N–O species **4**, typically formed through calcination in the presence of oxygen or *via* catalytic oxidation in air from the N–H species, can be readily converted to **5** (Scheme 5). Both species collaborate in an Ishii-type catalytic process (NHPI–PINO process) using oxygen as the oxidant.[17] XPS analysis of the current catalyst reveals the presence of the N–O species in the Cu_2O/C_3N_4 nanocomposite (Fig. 3b, 404.26 eV). Based on these, we hypothesize that the mechanisms involving TBHP and the circulation of N–O species coexist in the current Cu_2O/C_3N_4-catalyzed oxidation of benzyl ether.

Based on previous reports and the results presented above, we propose a plausible mechanism outlined in Scheme 6.[5e,16,17,18] When TBHP is used as the sole oxidant, the mechanism follows Path a, as shown in Scheme 4. In this pathway, Cu^{I} reacts with TBHP to form a *tert*-butoxy radical and a molecule of $Cu^{II}OH$. The *tert*-butoxy radical then interacts with compound **1**, abstracting the benzylic hydrogen atom to generate the benzylic radical **A**. Under the influence of $Cu^{II}OH$, radical **A** is transformed into the benzylic hydroxyl compound **B**, with Cu^{II} being reduced to Cu^{I} in the process. Subsequently, **B** is deprived of a hydrogen atom by another molecule of *tert*-butoxy radical, leading to the radical intermediate **C**. This intermediate further reacts with $Cu^{II}OH$, yielding a molecule of water and the final product, benzoate **2**.

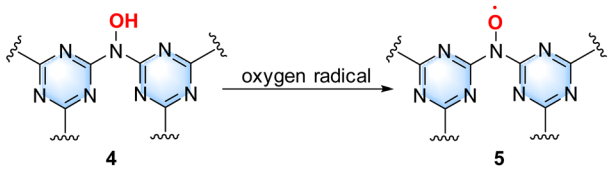

Scheme 5 The plausible N–O specie in the reaction.

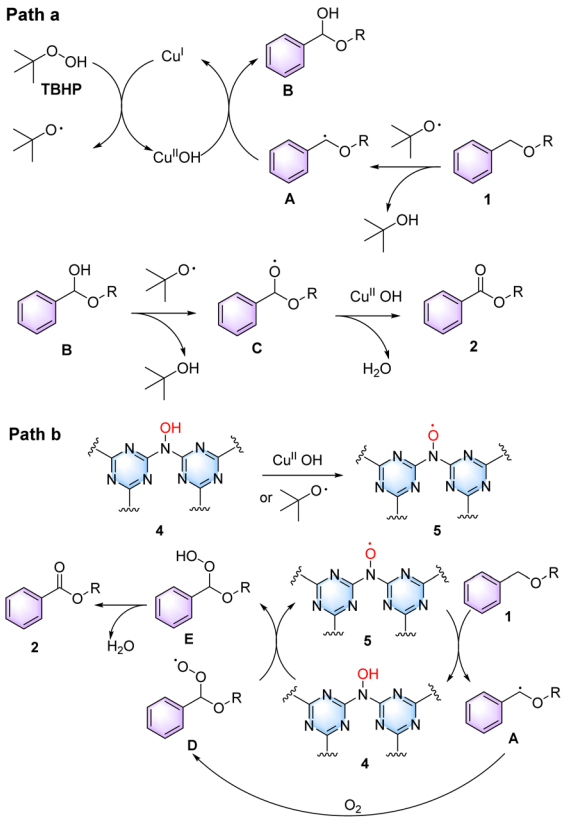

Scheme 6 The plausible mechanism: (a) the mechanism with TBHP as the oxidant; (b) the mechanism with oxygen as co-oxidation.

Path b in Scheme 4 elucidates an alternative mechanism where oxygen acts as an aiding oxidant. The *tert*-butoxy radical or $Cu^{II}OH$, generated by the reaction between Cu_2O and TBHP, efficiently transforms the N–O species **4** on the C_3N_4 into the N–O radical **5**, that explains why no reaction occurs in an O_2 atmosphere without TBHP (entry 8 in Table 1). Following the Ishii-type catalytic process, the N–O radical **5** abstracts a benzylic hydrogen atom from substrate **1**, producing the N–O species **4** and the benzyl radical **A**. In an air atmosphere, benzyl radical **A** reacts with oxygen to form the benzyl peroxy-radical **D**. When **D** captures a hydrogen atom from species **4**, it not only completes the cycle of the N–O species but also generates the benzylic hydroperoxide product **E**. Compound **E** readily loses a water molecule to yield the final product, benzoate **2**.

Conclusions

In summary, we demonstrated an efficient and selective oxidation process for benzyl ether utilizing a Cu_2O/C_3N_4 catalyst. Notably, the reaction was successfully carried out at room temperature with less than the required amount of TBHP as the oxidant, achieving yields between 75–97% for various substrates. Our mechanistic studies indicated that oxygen from the air synergistically acts as a co-oxidant with TBHP, aided by the N–O species contained within the N–C materials. This approach presents a promising, cost-effective, and environmentally friendly strategy for producing aromatic esters.

Data availability

The data supporting this article have been included as part of the ESI.†

Conflicts of interest

There are no conflicts to declare.

Acknowledgements

We are grateful to the financial support from National Natural Science Foundation of China (21772091 to X. Y.). This is a project funded by the Priority Academic Program Development of Jiangsu Higher Education Institutions.

Notes and references

1 B. Neises and W. Steglich, *Angew. Chem.*, 1978, **17**, 522.
2 Y. Bian, J. Zhang and S. Zhang, *ACS Sustain. Chem. Eng.*, 2019, **7**, 17220.
3 M. Oliverio, M. Nardi and L. Cariati, *ACS Sustain. Chem. Eng.*, 2016, **4**, 661.
4 S. P. Chavan, R. R. Kale and K. A. Shivasankar, *Synthesis*, 2003, **17**, 2695.
5 some recent examples: (*a*) W. Abudureheman, T. Xiarepati and C. D. Lu, *Eur. J. Org Chem.*, 2012, 3088; (*b*) T. Sastraruji, S. G. Pyne and A. T. Ung, *Tetrahedron*, 2012, **68**, 598; (*c*) P. Li, J. Zhao and R. Lang, *Tetrahedron Lett.*, 2014, **55**, 390; (*d*) N. Kato, Y. Hamaguchi, N. Umezawaa and T. Higuchi, *J. Porphyrins Phthalocyanines*, 2015, **19**, 411; (*e*) M. M. Hossain and S. Shyu, *Tetrahedron*, 2016, **72**, 4252; (*f*) L. C. Finney, L. J. Mitchell and C. J. Moody, *Green Chem.*, 2018, **20**, 2242; (*g*) T. Ye, Y. Li, Y. Ma, S. Tan and F. Li, *J. Org. Chem.*, 2024, **89**(1), 534.
6 (*a*) A. Shaabani, S. Shaabani and H. Afaridoun, *RSC Adv.*, 2016, **6**, 48396; (*b*) L. Ren, M.-M. Yang, C.-H. Tung, L.-Z. Wu and H. Cong, *ACS Catal.*, 2017, **7**, 8134; (*c*) J. Liu, C. Wan, A. Zheng, L. Wang, K. Yin, D. Liu, S. Wang, L. Ren and S. Gao, *Chin. J. Org. Chem.*, 2019, **39**, 811.
7 A very recent review: T. Muhmood, I. Ahmad, Z. Haider, S. K. Haider, N. Shahzadi, A. Aftab, S. Ahmed and F. Ahmad, *Mater. Today Sustain.*, 2024, **25**, 100633.
8 S. K. Verma, R. Verma, Y. R. Girish, F. Xue, L. Yan, S. Verma, M. Singh, Y. Vaishnav, A. B. Shaik, R. R. Bhandare, K. P. Rakesh, K. S. Sharath Kumar and K. S. Rangappa, *Green Chem.*, 2022, **24**, 438.
9 W. Lv, J. Tian, N. Deng, Y. Wang, X. Zhu and X. Yao, *Tetrahedron Lett.*, 2015, **56**, 1312.
10 (*a*) H. Xu, K. Wu, J. Tian, L. Zhu and X. Yao, *Green Chem.*, 2018, **20**, 793; (*b*) H. Xu, J. Wang, P. Wang, X. Niu, Y. Luo, L. Zhu and X. Yao, *RSC Adv.*, 2018, **8**, 32942; (*c*) H. Xu, L. Wu, J. Tian, J. Wang, P. Wang, X. Niu and X. Yao, *Eur. J. Org Chem.*, 2019, **39**, 6690.
11 (*a*) J. Guo, Y. Zhao, P. Wang, Y. Song, Y. Shao, L. Zhu and X. Yao, *J. Mater. Chem. A*, 2022, **10**, 11268; (*b*) Z. Liang, J. Guo, P. Wang, L. Zhu and X. Yao, *Chin. Chem. Lett.*, 2023, **34**, 108001.
12 A. Mitra, P. Howli and D. Sen, *Nanoscale*, 2016, **8**, 19099.
13 W. J. Ong, L. L. Tan and Y. H. Ng, *Chem. Rev.*, 2016, **116**, 7159.
14 (*a*) W. Chen, Z. Fan and Z. Lai, *J. Mater. Chem. A*, 2013, **1**, 13862; (*b*) B. Peng, S. Zhang, S. Yang, H. Wang, H. Yu, S. Zhang and F. Peng, *Mater. Res. Bull.*, 2014, **56**, 19; (*c*) B. Wang, L. Wu, A. Sun, T. Liu, L. Sun and W. Li, *New J. Chem.*, 2023, **47**, 13797.
15 Y. Hou, Z. Wen and S. Cui, *Adv. Mater.*, 2013, **25**, 6291.
16 S. Nie, J. Wang, X. Huang, X. Niu, L. Zhu and X. Yao, *ACS Appl. Nano Mater.*, 2018, **1**, 6567.
17 B. Saha, N. Koshino and J. H. Espenson, *J. Phys. Chem. A*, 2004, **108**, 425.
18 B. Gao, S. Meng and X. Yang, *Org. Process Res. Dev.*, 2015, **19**, 1374.